BME 355 Project

A Model of Functional Electrical Stimulation for Foot Drop

University of Waterloo

Faculty of Engineering

Charmaine Koo - ████████

Paige Lavergne - ████████

Cathleen Leone - ████████

Anne Mei - ██████

Natasha Willis - ███████

April 3, 2020

Prepared for Dr. Bryan Tripp

Abstract

Foot-drop is a common condition where gait is impaired due to weakness or paralysis of muscles in the foot, causing the inability to lift the foot during the swing phase of gait [1]. Functional electrical stimulation (FES) is a common treatment for foot-drop, where an electrical current targets the common peroneal nerve during dorsiflexion to achieve normal gait patterns. However, one limitation of FES is its tendency to cause rapid muscle fatigue. Thus, this report simulates a nonlinear musculoskeletal model of the leg, from knee to foot, in order to optimize FES parameters to reduce muscle fatigue. This was done by simulating the model using various pulse train stimulation signals, including three simple geometric pulse trains and one uniquely shaped signal. The final signal was generated based on expected values which would elicit a natural excitation response. Appropriate validation of the model and regression methods were carried out in order to ensure the accuracy of these results through the plotting of the state variable trajectories (ankle angle, angular velocity, and activation). A cost function was used to optimize the input signal by minimizing muscle fatigue and by maintaining natural gait patterns according to the remaining state variables, which showed that a uniquely generated pulse train stimulation signal was the most efficient at limiting fatigue during FES for foot-drop. This conclusion offers valuable insight into what types of stimulation signal shapes are most appropriate for the correction of foot-drop, while achieving a balance between attaining a natural gait pattern and limiting muscle fatigue.

Keywords: Functional Electrical Stimulation, foot-drop, musculoskeletal model, tibialis anterior, pulse train modifications

Table of Contents

Introduction

Foot-drop is a condition that is prevalent among stroke victims, patients with multiple sclerosis (MS), and Amyotrophic Lateral Sclerosis (ALS) [1]. Of the 15 million people who suffer from strokes each year worldwide, 20% of stroke survivors exhibit foot-drop [1]. Moreover, 90% of patients living with MS also exhibit foot-drop [2]. Foot-drop is an early symptom of ALS which is exhibited by 75-80% of those diagnosed [3]. Other causes of foot-drop such as proximal tibial osteotomy and nerve injuries, among others, account for 3-13% of all cases [4].

Foot-drop stems from a weakness or inability of the ankle flexor muscles to lift the foot and toes up during the swing phase of the walking cycle [5]. This leads the foot to drag on the ground, resulting in foot-drop [6]. Specifically, the ankle flexor muscles affected are the tibialis anterior, extensor hallucis longus, and extensor digitorum longus [7]. The most common causes of this disability are related to the nervous system, both central and peripheral [8]. In the peripheral nervous system, most issues arise from the lumbosacral plexus (L4-S1 nerves), which contains the nerves that provide information to the ankle flexor muscles by way of the peroneal nerve [6, 7]. When there is a lesion or growth that compresses these nerves, the signal from the brain to muscles is slowed or cut off based on the severity of the injury [6, 7]. Additionally, other possible causes include strokes, where the part of the brain which sends signals to the flexor muscles is damaged, as well as diseases that affect the myelin sheaths of nerves, which stop the electric signal from passing from nerve to nerve [6, 7].

Existing Solutions

Currently, there are many existing treatment methods currently available for foot-drop, including Ankle Foot Orthotics (AFO), Electromyographic Biofeedback (EMG-BFB), and Functional Electrical Stimulation (FES) [8, 9]. These treatments share a common goal of reducing muscle fatigue, lowering the incidence of falls, increasing confidence, and improving overall gait [9]. However, each treatment takes a different approach in achieving these objectives. An AFO is a mechanical brace that is commonly used to treat foot-drop and children with cerebral palsy who have abnormal gait [10]. The AFO is rigid and gives external support, including three-point pressure, to allow toe clearance for patients with foot-drop [10]. One limitation of the AFO is its rigidness, making it uncomfortable and reducing its ability to improve velocity of gait or stride length [10]. EMG-BFB has been used in rehabilitation for many types of physiological damage, including foot-drop after stroke [8]. From the body's physiological systems, biofeedback from the neuromuscular system can be measured and used for EMG-BFB, where new feedback systems are created to retrain the muscle of interest [11]. These feedback systems are generated by making visual and auditory signals, and the treatment is easy to repeat, implement, and gives the patient and physiotherapist continuous communication between them [12]. This treatment has mixed reviews, with some saying that it aids in increasing muscle strength and locomotion recovery, and others saying that it does not aid in paretic limb functional recovery [12]. FES is one of the most common treatments for foot-drop. It uses a tilt sensor attached to the shank-foot to detect each phase in the gait cycle and reacts accordingly to support dorsiflexion during the gait's swing phase [1, 9]. Dorsiflexion is enhanced by stimulating the damaged muscles with an electric current that targets the common peroneal nerve with electrodes, causing sufficient dorsiflexion to achieve normal gait [13]. One major limitation of FES is the tendency for muscles to fatigue more rapidly and intensely compared to natural muscle stimulation [14]. This is

because when a muscle is normally stimulated by a neural input, smaller motor units are recruited first, followed by larger and more motor units to control muscle force voluntarily [15]. Since FES stimulates motor units non-selectively, a larger force is often generated than what is required for dorsiflexion thus resulting in muscle fatigue [15].

Iterations of the technology have attempted to mitigate muscle fatigue by optimizing the stimulation model for FES. This is done by modifying parameters such as frequency of stimulation, signal waveform (asymmetrical vs. symmetrical), ramp up and ramp down, extension, pulse duration/width, and current amplitude [9, 16]. These modifications can influence the order of muscle fiber recruitment [9, 16]. It has been shown that FES patterns with relatively high-frequency pulse trains contribute to increased muscle fatigue [15, 17]. Furthermore, there is no set of optimal parameter values that work perfectly for each individual, as they vary with their movement patterns and comfort preferences. However, there is a recommended range of stimulation frequencies of 25-40Hz, which has been found to produce a smooth contraction with less muscle fatigue [9]. Pulse width is also typically set between 25 to 300μs [9]. A separate study used the mechanomyographic efficiency index to determine optimal FES parameters and concluded that a pulse frequency of 1kHz, pulse duration of 200μs, and burst frequency of 50Hz was the most efficient [18].

Project Goal

This project aims to develop a physiological model for a foot-drop assistive device. As FES is commonly used for these devices, a musculoskeletal model will be developed to optimize the FES parameters. The project goal is to minimize fatigue, as measured by a muscle activation-time integral, by modifying FES parameters such as duty cycle and different stimulation patterns, while ensuring that gait parameters such as ankle angle and angular velocity closely resemble natural curve-fitted trajectories, such that the RMSE between the simulated and curve-fitted natural trajectories is minimized.

Impact

While FES is a common treatment for foot-drop, it has limitations, including its causation of muscle fatigue [9]. By developing a musculoskeletal model for a foot-drop assistive device to optimize FES parameters in order to reduce muscle fatigue (as mentioned in the Project Goal), this limitation of FES could be mitigated. Thus, FES would become a more favourable treatment for foot-drop, and possibly be an integral part of treatments for other disorders such as spinal cord injury (SCI). With less muscle fatigue from FES, patients would experience reduced complications from muscle fatigue, leading to an increased quality of life.

Methods

Model Development

To create a model for the use of FES for the correction of foot drop, a system was developed in Python using state equations to create a predictive gait simulator. From research into the problem space and previously developed models, the following equations (shown in Equation 1) were taken from a non-linear model that aimed to correct foot drop using predictive control [20].

$$x = \begin{bmatrix} x_1 \\ x_2 \\ x_3 \end{bmatrix} = \begin{bmatrix} f_{act} \\ \alpha_f \\ \alpha_F \end{bmatrix} \quad \dot{x} = \begin{bmatrix} \dot{x_1} \\ \dot{x_2} \\ \dot{x_3} \end{bmatrix} = \begin{bmatrix} (u(t) - x_1)(\frac{x_1}{T_{act}} - \frac{1-u(t)}{T_{deact}}) \\ x_3 \\ \frac{1}{J}(F_m(\boldsymbol{x}, u(t))d + T_{grav}(x_2) + T_{acc}(x_1{}^{ext}, x_2{}^{ext}, x_2) + T_{Ela}(x_2) + B(x_4{}^{ext} - x_3)) \end{bmatrix} \tag{1}$$

In this state vector, the x_1 value represents the normalized value of the dynamic activation level of the tibialis anterior muscle [20]. The x_2 value represents the absolute orientation of the shank foot with respect to the horizontal axis in the counterclockwise direction [20]. Finally, the x_3 value represents the rotational velocity of the shank foot in the same axis as x_2 [20]. Finding the derivatives of the entire state vector allows for the determination of each variable's rate of change to allow the development of a simulated trajectory over the gait cycle.

This system is controlled with an input vector $u(t)$ which is equal to $\varepsilon(t)$, where $\varepsilon(t)$ represents muscle excitation in a normalized range of $0 \le \varepsilon(t) \le 1$ [20]. For the purposes of this project, the input $u(t)$ was modified from the literature to be a function of time, rather than a constant, to allow modification of stimulus parameters such as signal shape, in an effort to reduce the amount of fatigue experienced by the tibialis anterior muscle.

As seen in the equation for the derivative of x_3, the equation for the muscular force of the tibialis anterior is used. This equation is the product of muscle activation, maximal isometric force of the muscle, and the parameters f_{fl} and f_{fv}. The variable f_{fl} represents the nonlinear relationship between the generated force and the length of the tibialis muscle which is calculated based on the length of the contractile element of the muscle at a given ankle angle [20]. The variable f_{fv} is the non-linear force velocity relationship between the muscle force and the contraction speed of the muscle, which has a different computation if the muscle is contracting or extending [20]. The equations for these two variables are shown below in Equation 2, where l_{CE} is the length of the contractile element, W is a shape parameter, v_{CE} is the contraction speed, v_{max} is the maximum contraction speed.

$$f_{fl}(x_3{}^{ext} - x_2) = \exp\left(-\left[\frac{l_{CE} - l_{CE,opt}}{W l_{CE,opt}}\right]^2\right)$$

$$f_{fv}(x_4{}^{ext} - x_3) = \frac{1 - \frac{v_{CE}}{v_{max}}}{1 + \frac{v_{CE}}{v_{max} * f_{v1}}} \quad if \; v_{CE} < 0$$

$$f_{fv}(x_4{}^{ext} - x_3) = \frac{1 + a_v \frac{v_{CE}}{f_{v2}}}{1 + \frac{v_{CE}}{f_{v2}}} \quad if \; v_{CE} < 0 \tag{2}$$

Additionally, there are other factors that affect the ankle joint and thus the model that is attempting to be simulated, such as torque and viscosity. In the equation for x_3, the torques that are utilized are the torque induced by the movement of the ankle (T_{acc}), the torque induced by the gravity acting on the foot (T_{grav}) and the torque of the passive elastic muscles and tissues around the ankle (T_{Ela}) [20]. To simplify the model, the T_{Ela} term was removed from the state

equation for x_3 since the effects are considered negligible, and the torque was calculated to be constant at any given time or input [20]. Finally, the viscosity parameter, B, allows for the calculation of the relative angular velocity of the ankle joint when used in conjunction with the $(x_4{}^{ext} - x_3)$ value [20].

The external state vector, x^{ext}, consists of the sagittal and vertical linear accelerations of the ankle, as well as the absolute position and velocity rotation of the shank. This state vector is considered external since it is outside of the system boundaries, however, the trajectories of the external state variables are necessary as inputs to the system. The trajectories were obtained by extracting data for $a_{x,A}$, $a_{z,A}$, and α_S from various research papers using WebPlotDigitizer [20, 21]. The data for $\dot{\alpha}_S$ was obtained through numerical differentiation of α_S. The data was then curve-fitted using a linear regression with Gaussian basis functions to use in the simulation model. The means and variances of the Gaussian basis functions were determined experimentally with evenly spaced means, 0.05 units apart, with variances of 0.05, which were determined to reduce root mean squared error (RMSE) between the curve-fit and the original data. This regression method was used for curve fitting of other trajectories, such as expected state trajectory results, with different basis function parameters, in order to minimize RMSE. The resulting curve-fits were used as additional inputs to the system where applicable.

As foot drop is caused by a weakness or lack of signal travelling to the tibialis anterior (TA) muscle, the activation can be modelled using the muscle movement on the lower leg and ankle from the toe-off section of the gait phase, shown in Figure 1 [20]. In terms of system boundaries, the model focuses solely on the shank, foot, and dorsiflexion muscles (especially the TA), meaning that the plantar flexion muscles and upper part of the leg are not included in this model. As the model focuses solely on dorsiflexion, we can accurately model ankle angle and angular velocity as there will be no interference from the plantar flexion muscles. The force F_m in Figure 1 is the force from the electrically stimulated TA muscle, which controls the foot's relative orientation with respect to the shank. Both α_F and α_S allow for absolute orientations as they are the angles of the foot/shank with respect to the horizontal/vertical axis, respectively (positive in the counterclockwise direction).
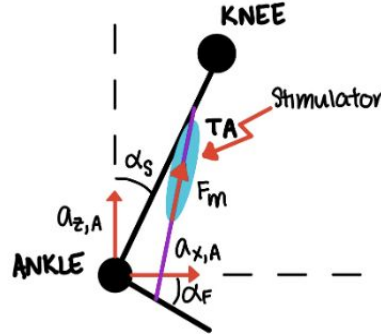

Figure 1: Model of FES simulated gait [20]

In order to evaluate the effect of changing FES signal parameters, such as pulse-width and signal shape, the signal must be translated to an excitation signal in order to be inputted to the model. In this investigation, we will maintain a constant signal frequency of 35 Hz, since it has been shown that frequencies between 30-35 Hz typically reduce fatigue while allowing for sufficient force generation [22, 23]. By maintaining a constant stimulation frequency, we will observe the effects of different signal shapes on muscle fatigue and ankle angular motion. Changing the shape of the

signal involves modifying the pulse-width, which is proportional to stimulus intensity, over time. Thus, the dependent variable for the FES signal will be signal pulse-width, in microseconds. The pulse width can be modified at discrete points in time, as dictated by the signal frequency.

   To test the model for accuracy and develop an optimized FES signal that will allow for the natural gait cycle to be achieved for a person with drop foot, three different FES stimulation signal shapes can be used to test its similarity to the expected results for the model. The first signal to be tested was a generic rectangular signal, as that is the most basic signal that can be developed. The second signal was a triangular shaped pulse which would represent a ramp up of pulse-width followed by an immediate and equal drop off in pulse-width. The next signal combined the two previous signals by using a trapezoidal signal shape, which is a commonly used FES signal shape. This signal incorporated the ramping up and down of the signal at the beginning and end of the toe-off section of the gait cycle and allowed for maximum pulse-width to be used for an extended period of time. The tested signals are depicted in Figure 2.
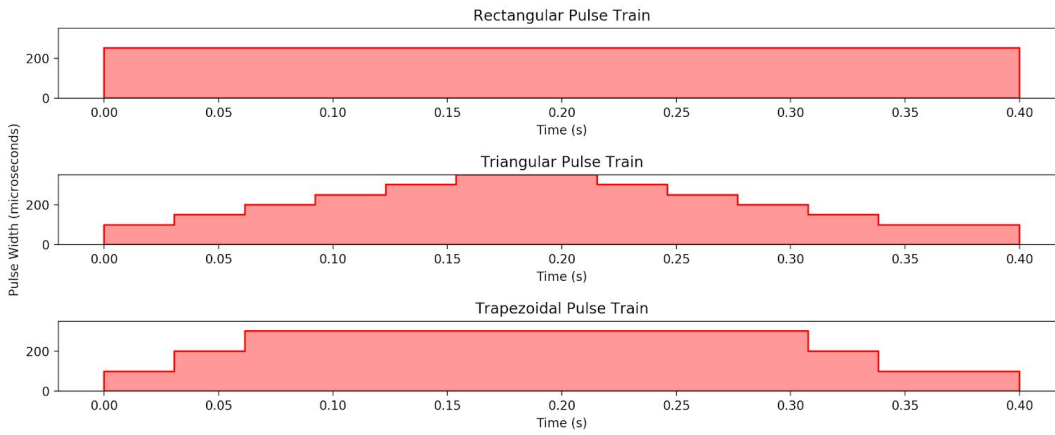

Figure 2: Three FES signal shapes to be tested: rectangular, triangular, and trapezoidal

In order to evaluate these signals in terms of the produced activation, ankle angle, and angular velocity, they must be translated to a muscle excitation signal, which is the input to the proposed model. To map these signals from the input FES pulse train to a muscle excitation, excitation data for the TA muscle corresponding to varying pulse widths presented by O'Keefe et. al. will be used [22]. The excitation corresponding to a given pulse-width is also dependent on the ankle's angular position, as it was found that a constant pulse-width FES signal produced varying EMG measurements depending on the ankle angular position [22]. For example, at a pulse width of 300μs, the excitation measured in the TA will be 0.62 at an angle of 13 degrees, however the excitation at the same pulse width but an angle of -1 degrees was measured to be 0.78. Therefore, for a given ankle angle and pulse-width, the excitation can be determined using a lookup table based on the data presented in Figure 3. Once the excitation data has been obtained from the lookup table, the data will be curve-fitted using a linear regression with Gaussian basis functions to produce the excitation signal.

Pulsewidth Angle (Degrees)	100μs RMS (Norm)	150μs RMS (Norm)	200μs RMS (Norm)	250μs RMS (Norm)	300μs RMS (Norm)	350μs RMS (Norm)	400μs RMS (Norm)
-16	0.107	0.28	0.45	0.515	0.548	0.44	0.37
-15	0.115	0.28	0.48	0.542	0.57	0.46	0.38
-14	0.11	0.295	0.51	0.562	0.585	0.49	0.4
-13	0.115	0.3	0.58	0.595	0.62	0.49	0.44
-12	0.117	0.305	0.64	0.608	0.645	0.5	0.47
-11	0.116	0.325	0.665	0.62	0.67	0.51	0.49
-10	0.115	0.34	0.7	0.635	0.7	0.54	0.5
-9	0.115	0.375	0.72	0.66	0.72	0.59	0.51
-8	0.115	0.4	0.725	0.689	0.725	0.62	0.53
-7	0.112	0.45	0.74	0.71	0.725	0.63	0.54
-6	0.11	0.45	0.76	0.745	0.735	0.65	0.59
-5	0.11	0.47	0.79	0.765	0.74	0.68	0.63
-4	0.112	0.49	0.8	0.785	0.745	0.72	0.65
-3	0.115	0.51	0.805	0.79	0.75	0.76	0.65
-2	0.119	0.53	0.814	0.8	0.76	0.8	0.65
-1	0.12	0.55	0.82	0.82	0.78	0.84	0.67
0	0.125	0.58	0.83	0.89	0.79	0.86	0.7
1	0.14	0.6	0.8	0.97	0.81	0.88	0.76
2	0.147	0.65	0.77	0.98	0.83	0.89	0.76

Figure 3: Lookup table for determining the pulse width of the TA excitation signal [22]

To produce the most promisingly optimal FES signal to mimic natural physiological motion, the lookup table can also be used to determine the optimal pulse-width for a given ankle angular position and excitation level. Following the trajectory for natural muscle excitation and corresponding angular position, another lookup table can be generated to determine the desired pulse-width for a given excitation level and ankle angular position, thus generating a uniquely shaped FES signal. For example, based on the data in Figure 3, following natural trajectories for ankle angle and TA excitation, at toe-off the angle would be -15 degrees while the TA excitation would be about 0.48, thus according to the data, a suitable pulse width for point in the FES signal would be 200 μs [22]. This method was employed to produce a unique FES signal shape, as shown in Figure 4.
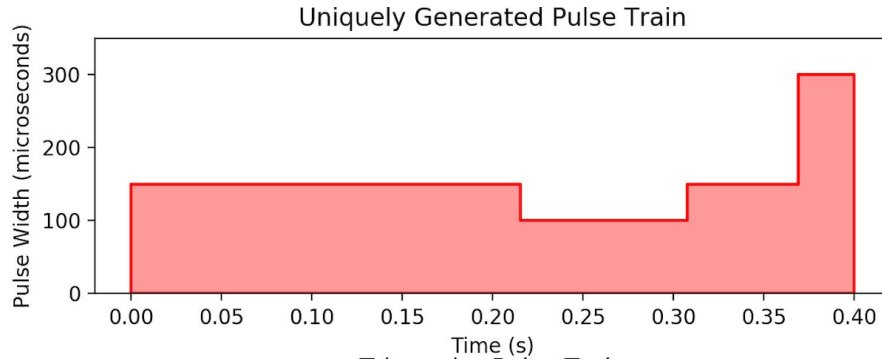

Figure 4: Uniquely Generated FES Signal Shape

Analysis and Validation

Once the excitation values have been passed to the simulated TA model, the state variables will be plotted against the expected natural values to observe which of the simulated pulse trains generates results that are most similar to the natural gait cycle. To quantitatively evaluate the similarity of the FES-induced trajectories for ankle angle and angular velocity to natural trajectories, the area between the simulated trajectory and natural trajectory can be calculated via integration. To quantitatively evaluate muscle fatigue for a given excitation signal, the fatigue

can be assumed to be related to the activation-time integral, since activation is proportional to force. The different signals u(t) will be ranked as to which one minimizes both the muscle activation-time integrals and the error between simulated and experimental ankle angle and angular velocity, thus achieving the most natural gait movement while minimizing fatigue. This is achieved by minimizing a cost function, shown in equation 3 below.

$$\int_0^{0.4} (c_1 f_{act}(t) + c_2 |\alpha_{FS}(t) - \alpha_{FE}(t)| + c_3 |\dot{\alpha}_{FS}(t) - \dot{\alpha}_{FE}(t)|) dt$$
(3)

Here, the subscripts *S* and *E* represent simulated and experimentally found values for natural motion, respectively, and $c_i \in [0, 1]$ are the corresponding costs for each state variable to normalize and scale them accordingly based on importance.

Validation of the model is necessary to ensure the model is behaving reasonably and meets the purposes it was originally designed for. The initial project goal was to develop a model that optimizes parameters in a way to reduce fatigue as well as to ensure ankle angle and angular velocity parameters have a trajectory that is similar to natural gait.

To validate that the model is behaving reasonably, various sanity checks can be performed. First, when stimulation frequency and amplitude increase, the TA activation, ankle angle, and angular velocity should all increase. When the activation graph has a decreasing slope, the angular velocity during that time should also be decreasing. Further, the relationship between the ankle angle and angular velocity graphs should be clear, such that the slope of the ankle angle graph should correlate to the angular velocity value at that point in time. Additionally, another sanity check can be implemented where the model is given a zero-excitation input, which should cause there to be no activation in the TA muscle meaning that the ankle angle and angular velocity should exhibit no angular change relative to the shank.

To validate the proposed model, all three state trajectories can be simulated using a similar input that was used in the literature source, to ensure that the results are similar and that the model is working properly. To do so, the simulated trajectories and the ones obtained from the literature source should be plotted in an overlayed manner to compare them. Then, the normalized root mean squared error can be calculated for the two sets of data to obtain a numerical value of their difference. The RMSE was normalized based on the range of the dependent variable, in order for the error in each trajectory to be comparable. There is some error that is expected between the results obtained from literature, and the simulated results, because there will be slight differences in the input signal, as well as due to the fact that different numerical integration techniques were used. The model can be considered acceptable for this validation check if the three NRMSE values are in a similarly low range.

Assumptions and Limitations

One assumption for this model is that contact forces on the leg are insignificant during the swing phase. This is because antagonistic muscles are not activated during the swing phase, but could be activated during push off. Another assumption is that there is a constant tendon length, which allows for the finding of the muscle length, and thus the length of the contractile element. Another assumption is that the swing phase of the gait cycle has a duration of 0.4 s. The final assumption is that the model is for a healthy adult leg that responds to stimuli in an average manner. This would result in the limitation that the model can only simulate the muscles to function as an average healthy adult leg would.

Results

After generating the various FES pulse train signals, the excitation inputs were determined and the simulation was run for 0.4 seconds to model the dorsiflexion section of the walking cycle, between toe-off and heel-strike. The first simulation that was performed was to validate the model by inputting a similar excitation signal as from the original literature source. Figure 5 a) shows the comparison of the simulated trajectories and the trajectories obtained from literature, while b) shows the same comparison without the first 0.1 seconds of simulation. This was done to remove the large peaks in the literature data at the beginning of the signals which were not handled well by the numerical integration technique employed for simulation. For both, the NRMSE was calculated between the simulated trajectories and the trajectories from literature.
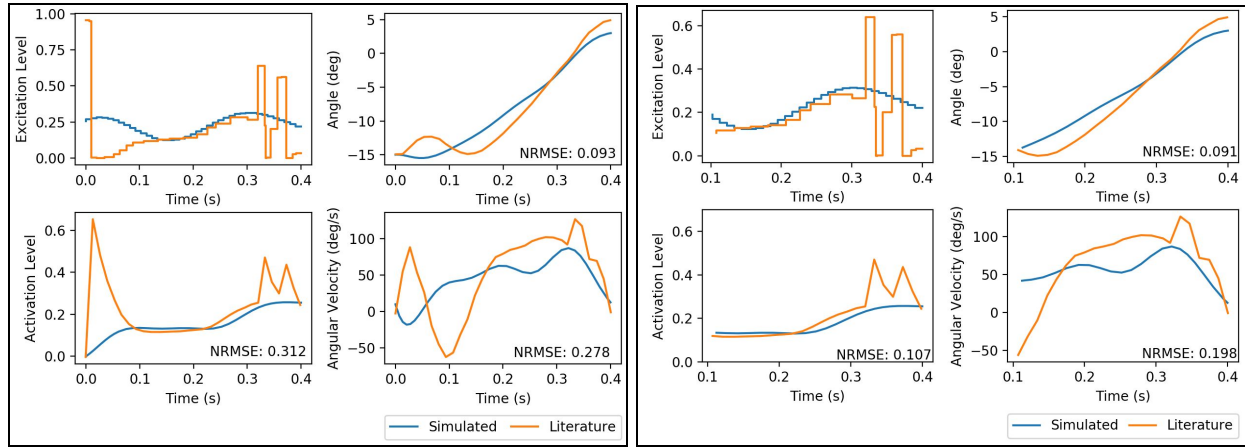

Figure 5: a) Comparison of literature and simulated trajectories (left)
b) Truncated comparison (right)

With each of the four excitation signal shapes shown in Figure 6 a) below, the corresponding generated excitation signals are plotted over each other to view the overall produced shape and compare the differences. Figure 6 b) shows that the excitation signal produced using the unique signal is the closest to a natural excitation shape. In contrast, the excitation signals generated from the rectangular, triangular, and trapezoid pulse trains all have a parabolic shape.
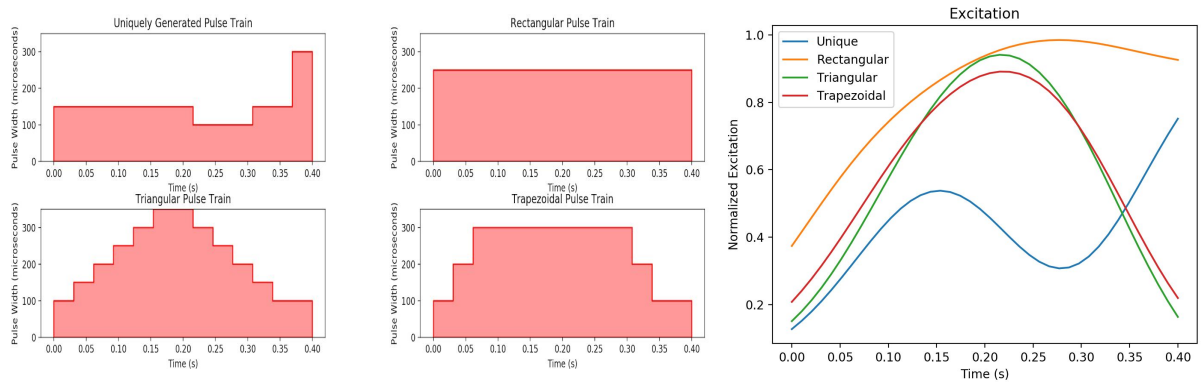

Figure 6: a) FES stimulation signals and b) corresponding excitation signals obtained from regression model

Figure 7 a) and b) below show the activation curves for the various pulse train signals that have been passed through the model and a comparison of the activation trajectories and activation-time integrals. As expected, the activation-time integral was the smallest for the unique pulse train signal meaning that the fatigue is expected to be lowest for this FES signal shape.
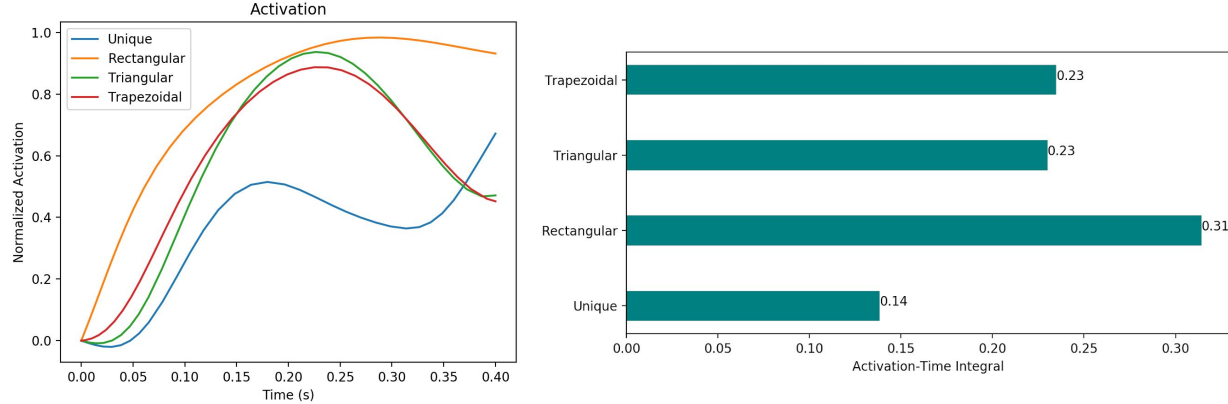

Figure 7: a) Activation trajectories, and b) activation-time integrals for various input signals

A curve-fitted plot for the natural ankle angle trajectory, shown in Figure 8 b) was generated by passing extracted sample data found in a literature paper, shown in Figure 8 a), into a linear regression model with Gaussian basis functions. The regression produced a normalized RMSE (NRMSE) of 0.037.
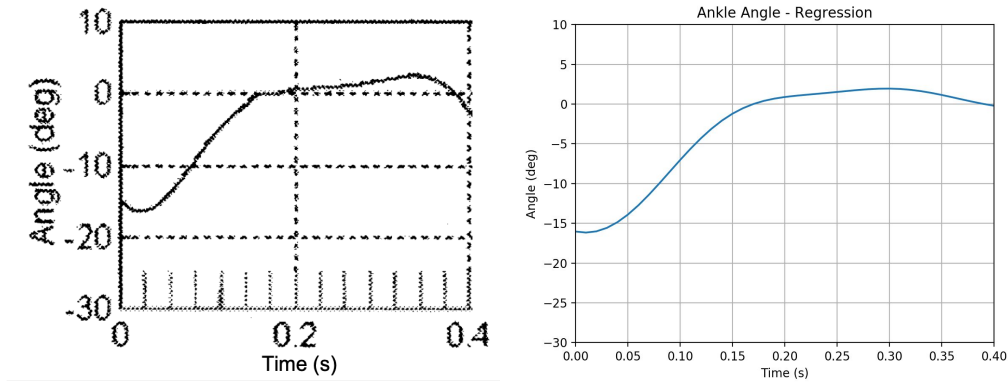

Figure 8: a) Ankle angle data for toe-off from literature [22], and b) regression plot from model

In Figure 9 below, the trajectories for ankle angle, shown in Figure 9 a), and ankle angular velocity, shown in Figure 9 b), were obtained from the model state equations for each FES stimulus shape. The results were plotted against natural ankle angle and angular velocity trajectories.
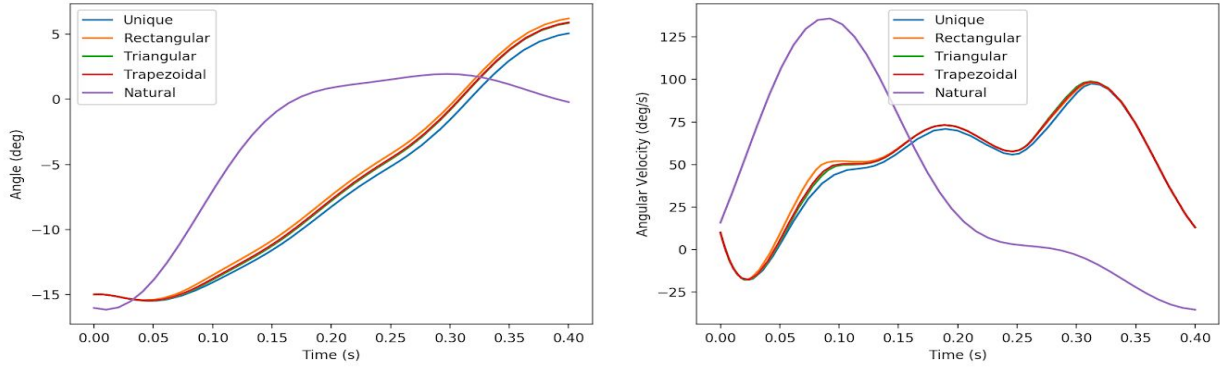
12

Figure 9: Plots of state variables for the various pulse trains a) ankle angle b) angular velocity

To evaluate the performance of each FES signal shape, the simulation results were used to calculate the relative cost for each signal according to Equation 2, with the goal of minimizing cost. The cost function results for each signal shape are summarized in Table 1 where the cost weight values used were $c_1 = 1$, $c_2 = 0.5$, $c_3 = 0.25$ for the activation, ankle angle and angular velocity respectively.

Table 1: Results of Cost Function

Signal Shape	Cost
Unique	1.11
Rectangular	1.75
Triangular	1.50
Trapezoidal	1.47

Discussion

Interpretation of Results

When examining the plots shown in Figure 5 in the results section, it can be seen that, while there is a considerable amount of similarities between the results of our simulation and the literature, there are also some differences in the plotted trajectories. There are a variety of reasons why this could have occured. The simulation technique used in the literature was not specified, meaning that we were not able to ensure the accuracy of our replication of their results in terms of the method of simulation. Our simulation was developed using the RK45 method, as implemented in the scipy.integrate.solve_ivp() python function. Certain differences can be expected given that different simulation methods were likely used.

Furthermore, it was noticed that large spikes or drastic changes in excitation inputs caused our simulation to respond differently compared to the results presented in the literature. Conversely, when the excitation input remained more stable over time, with more gradual growth of peaks, the trajectories of our simulation mimicked those of the literature with much greater accuracy. For this reason, the excitation signal used in the simulation was averaged at the locations of large spikes, and is not exactly the same as the literature signal. This could again be due to the different methods of numerical integration, as well as being affected by factors such as smoothening, curve fitting, or choice of time step. In order to deal with these anomalies, the first

peak of each dataset was omitted, preventing a large spike from impacting the excitation trajectory, and the final two drastic peaks were averaged to evaluate performance. These changes reduced the corresponding NRMSE values, and their trajectories can be seen in Figure 5 b). These NRMSE values and the relatively accurate trajectories confirm the validity of our model, given that the input excitation signal must not have drastically changing peaks. This is a reasonable and acceptable constraint due to the fact that the types of drastic changes in excitation which are problematic for our model are also uncharacteristic of natural muscle excitation.

The excitation plots generated using the four various FES signal shapes behaved as expected, as shown in Figure 6 in the results section. For the triangular and trapezoidal excitation, the plot shows a parabolic shape which corresponds to the ramp up and ramp down in the magnitude of the pulse width. The rectangular excitation curve also behaves as expected as the excitation increases and plateaus once the maximum excitation has been reached. The plot obtained using the unique pulse train being the closest to the results found in literature as shown in Figure 5 b). This similarity is due to the fact that the expected results were used in the development of the unique signal, therefore it should mimic the natural excitation most accurately. Since the expected results were obtained for the excitation, it can be assumed that the excitation data that is passed into the simulation model was as desired.

As mentioned in the introduction, FES has limitations including muscle fatigue, and optimization of personalized parameters. The clinical problem that the model developed addresses is the limitation of muscle fatigue. FES tends to cause muscle fatigue more rapidly than natural muscle stimulation due to FES stimulating motor units non-selectively, which generates a larger force than needed for dorsiflexion. This greater force causes muscle fatigue to occur more rapidly. As one of the project goals was to create a model to simulate the tibialis anterior to correct drop foot while reducing the fatigue in the muscle, Figure 7 was necessary to determine which of the generated pulse train signals was optimized. As the rectangular, triangular and trapezoidal signals have parabolic shaped activation curves, it makes sense that their activation-time integrals were larger than the cubic shaped curve of the unique signal. Since the activation-time integral is closely related to the fatigue of a muscle, one can determine that since the unique signal had a value of 0.14 compared to the other signals values of 0.23, 0.23 and 0.31 that the unique signal will decrease the fatigue in the tibialis anterior if it were to be used as the FES excitation signal.

In order to evaluate similarities between the simulated trajectories for ankle angle and ankle angular velocity, it is desirable to perform a curve-fit for the natural trajectories in order to predict the value of the natural trajectory at specific time points. A regression was also used to generate curve-fits for excitation signals given data obtained from the lookup table (Figure 3), for various FES inputs. Both curve-fits were obtained using a linear regression with Gaussian basis functions. The normalized RMSE was calculated for the curve-fit of the natural ankle angle trajectory, yielding a relatively low result of 0.037, indicating a good fit and thus validating the regression technique. The regression is shown in Figure 8 b), and visually reproduces the original data in Figure 8 a) as well.

Using these ankle angle and angular velocities, Figure 9 was generated in order to examine how the trajectories varied as a result of different pulse trains. In Figure 9 a), the ankle angle trajectories reveal that the ankle angles for the various pulse trains used for these simulations are extremely similar, while all being somewhat different from the natural ankle angle trajectory. When investigating the angular velocity trajectories, as seen in Figure 9 b), it

can be seen that the natural trajectory reaches its maximum much earlier than the other trajectories, and then continues to fall below these other trajectories. Conversely, the trajectories which use various different pulse trains experience a steady increase over time. Among these trajectories, there are very few differences, with all FES signals having similar impacts on the angular velocity trajectories.

The use of a cost function allows the relative importance of different factors and parameters to be taken into consideration when determining the optimal pulse train signal. The cost function is used by finding the parameters which result in the minimum cost value, using cost weight variables for each parameter to indicate which parameters are most important in the optimization process. For the purposes of this project, the highest cost weight variable of 1 was assigned to minimizing the activation-time integrals, due to the fact that this addresses a main goal of the project to reduce fatigue. The ankle angle and ankle angular velocity trajectories were then assigned cost weight variables of 0.5 and 0.25, respectively. Implementing the cost function in this manner ensures that the cost will be optimized in such a way that the greatest importance is placed on reducing muscle fatigue during FES, while consideration is still being given to maintaining a natural gait pattern through the optimization of ankle angle and ankle angular velocity.

It was also deemed to be more important than the angle and velocity trajectories because all signal shapes exhibited similar trajectories. Angle was considered to be more important than velocity, because it is more important to ensure the toe attains a proper clearance than the actual motion/velocity of dorsiflexion. As shown in Table 1, the uniquely shaped FES signal had the lowest result upon computing each cost function. It was also observed that when comparing each of the simulated trajectories with the natural trajectories, the unique signal had a slightly lower error between the expected and simulated ankle angle and angular velocity, as well as the lowest activation-time integral. The trapezoidal and triangular shaped signals produced comparable results, and were the second most optimal results, while the rectangular signal produced the highest cost function result.

Conclusions

When various signal shapes were evaluated as an FES stimulus signal, the uniquely generated pulse train signal based on a natural excitation trajectory produced simulated trajectories that most closely resembled natural physiological results. With this stimulation signal, the model also produced the lowest cost function in comparison to the other signal shapes, indicating the minimization of an activation-time integral, and close resemblance to natural trajectories for ankle motion. This would ultimately translate to the lower level of fatigue that an individual experiences when using a FES device programmed to provide the same signal shape that was reported.

Fatigue is an issue experienced by users of FES devices, as simulations that do not fit the user's unique walking patterns and muscles can lead to the TA muscle being simulated in a way that makes them feel fatigued after short periods of simulation. This is limiting because the individual then has to take frequent breaks. As such, reducing TA fatigue was set as one of the main goals for this project. Since the model was used to determine optimal parameters for the simulation that would also minimize fatigue, it was deemed that the goals set for the project were successfully met. The model can thus be used to represent the behaviour of an individual's

muscle and ankle behaviour when simulated with a FES device, by producing visual plots for the TA activation, ankle angle, and ankle angular velocity throughout the simulation. Due to time constraints, certain aspects of the model can also be further refined and improved to make it more efficient and accurate.

Recommendations

In terms of future recommendations for finding the optimal FES signal to reduce fatigue for drop foot, while closely mimicking natural gait, there are ways to improve this model. For the improvement of the model described in this report, more research can be done into tests that have modelled similar FES signals in order to investigate the resulting fatigue presented in each model. The fatigue level determined in our model could then be compared to the pre-existing data. Ideally, a t-test would be performed to examine whether or not there is a statistically significant difference in fatigue data between our model and models from past research. The results of this t-test would help confirm, in a statistically sound manner, whether or not our model was successful in meeting the objective of reducing fatigue during FES. Another recommendation is to rework the model or simulation techniques to allow for better handling of sharp input peaks shown in Figure 5 to be passed through the simulation as currently, the model does not perform well when faced with such patterns. One way of meeting this goal would be to find out which numerical integration method was used in past literature, and implement that method within our own model, rather than simply assuming that the RK45 method would provide accurate replications of existing simulations. Additionally, an alternative model could be found to take the FES stimulation signal directly as an input, rather than muscle excitation, thus reducing the computational complexity required to convert the FES signal to an excitation signal which can be used in the model. A final suggestion would be to incorporate the properties and behaviour of the soleus into the model. It provides resistance to dorsiflexion, but this resistance has been set to 0 in the model so that it has no impact on the dorsiflexion muscle. If the soleus were added, the model could be more accurate in its representation of an actual ankle of an individual who uses a FES device.

References

[1] P. Melo, M. Silva, J. Martins and D. Newman, "Technical developments of functional electrical stimulation to correct drop foot: Sensing, actuation and control strategies", *Clinical Biomechanics*, vol. 30, no. 2, pp. 101-113, 2015. Available: https://www.sciencedirect.com/science/article/pii/S0268003314002757. [Accessed 16 January 2020].

[2] H. Karpatkin, E. Euaparadorn and R. Schreyer, "Foot drop in MS: Evaluation and Treatment", *MScare.org*, 2014. [Online]. Available: https://cdn.ymaws.com/www.mscare.org/resource/resmgr/2014amslides/AllPresenters-Foot_drop_CMSC.pdf. [Accessed: 18- Jan- 2020].

[3] C. Armon and N. Lorenzo, "Amyotrophic Lateral Sclerosis: Practice Essentials, Background, Pathophysiology", *Emedicine.medscape.com*, 2018. [Online]. Available: https://emedicine.medscape.com/article/1170097-overview. [Accessed: 19- Jan- 2020].

[4] G. Majeed, M. Iedani and F. Aaqail, "The Role of Tibialis Posterior Tendon Transfer in Correction of Foot Drop Deformity", *Al Kinda College Medical Journal*, vol. 9, no. 2, pp. 86-69, 2013. Available: https://www.iasj.net/iasj?func=fulltext&aId=86342. [Accessed 18 January 2020].

[5] J. Stewart, "Foot drop: where, why and what to do?", *Practical Neurology*, vol. 8, no. 3, pp. 158-169, 2008. Available: http://dx.doi.org/10.1136/jnnp.2008.149393. [Accessed 17 January 2020].

[6] C. Aldemir and F. Duygun, "New and unusual causes of foot drop", *Medicine Science International Medical Journal*, vol. 6, no. 3, 2017. Available: https://www.ejmanager.com/mnstemps/53/53-1489048115.pdf?t=1578922382. [Accessed 17 January 2020].

[7] S. Daniels, J. Feinberg, J. Carrino, A. Behzadi and D. Sneag, "MRI of Foot Drop: How We Do It", *RSNA*, vol. 289, no. 1, 2018. Available: https://pubs.rsna.org/doi/full/10.1148/radiol.2018172634. [Accessed 18 January 2020].

[8] A. Carolus, M. Becker, J. Cuny, R. Smektala, K. Schmieder and C. Brenke, "The Interdisciplinary Management of Foot Drop", *Etsch Arztebl Int*, vol. 116, no. 20, pp. 347-354, 2019. Available: https://www.ncbi.nlm.nih.gov/pmc/articles/PMC6637663/. [Accessed 18 January 2020].

[9] A. Majid, *Electroceuticals: advances in electrostimulation therapies*, 1st ed. Cham: Springer, 2017.

[10] W. Lam, J. Leong, Y. Li, Y. Hu and W. Lu, "Biomechanical and electromyographic evaluation of ankle foot orthosis and dynamic ankle foot orthosis in spastic cerebral palsy", Gait & Posture, vol. 22, no. 3, pp. 189-197, 2005. Available: 10.1016/j.gaitpost.2004.09.011 [Accessed 31 March 2020].

[11] O. Giggins, U. Persson and B. Caulfield, "Biofeedback in rehabilitation", Journal of Neuroengineering and Rehabilitation, 2020. Available: https://www.ncbi.nlm.nih.gov/pmc/articles/PMC3687555/pdf/1743-0003-10-60.pdf. [Accessed 31 March 2020].

[12] D. Intiso, V. Santilli, M. Grasso, R. Rossi and I. Caruso, "Rehabilitation of walking with electromyographic biofeedback in foot-drop after stroke", *Stroke*, vol. 25, no. 6, pp. 1189-1192, 1994. Available: https://www.ahajournals.org/doi/abs/10.1161/01.str.25.6.1189. [Accessed 17 January 2020].

[13] M. Alam, I. Choudhury and A. Mamat, "Mechanism and Design Analysis of Articulated Ankle Foot Orthoses for Drop-Foot", *Scientific World Journal*, vol. 20, no. 14, 2014. Available: https://www.ncbi.nlm.nih.gov/pmc/articles/PMC4032669/. [Accessed 18 January 2020].

[14] D. Bhatia, G. Bansal, R. Tewari and K. Shukla, "State of art: Functional Electrical Stimulation (FES)", *International Journal of Biomedical Engineering and Technology*, vol. 5, no. 1, p. 77, 2011. Available: 10.1504/ijbet.2011.038474 [Accessed 20 January 2020].

[15] N. Malešević, L. Popović, L. Schwirtlich and D. Popović, "Distributed low-frequency functional electrical stimulation delays muscle fatigue compared to conventional stimulation", *Muscle & Nerve*, vol. 42, no. 4, pp. 556-562, 2010. Available: 10.1002/mus.21736 [Accessed 20 January 2020].

[16] A. Thrasher, G. Graham and M. Popovic, "Reducing Muscle Fatigue Due to Functional Electrical Stimulation Using Random Modulation of Stimulation Parameters", *Artificial Organs*, vol. 29, no. 6, pp. 453-458, 2005. Available: 10.1111/j.1525-1594.2005.29076.x [Accessed 20 January 2020].

[17] Z. Cai, E. Bai and R. Shields, "Fatigue and non-fatigue mathematical muscle models during functional electrical stimulation of paralyzed muscle", *Biomedical Signal Processing and Control*, vol. 5, no. 2, pp. 87-93, 2010. Available: 10.1016/j.bspc.2009.12.001 [Accessed 20 January 2020].

[18] E. Krueger-Beck, E. Scheeren, G. Nogueira-Neto, V. Button and P. Nohama, "Optimal FES parameters based on mechanomyographic efficiency index", *2010 Annual International Conference of the IEEE Engineering in Medicine and Biology*, 2010. Available: 10.1109/iembs.2010.5626735 [Accessed 20 January 2020].

[19] R. Stein et al., "Long-Term Therapeutic and Orthotic Effects of a Foot Drop Stimulator on Walking Performance in Progressive and Nonprogressive Neurological Disorders", *Neurorehabilitation and Neural Repair*, vol. 24, no. 2, pp. 152-167, 2009. Available: https://journals.sagepub.com/doi/pdf/10.1177/1545968309347681. [Accessed 20 March 2020].

[20] M. Benoussaad, K. Mombaur and C. Azevedo-Coste, "Nonlinear model predictive control of joint ankle by electrical stimulation for drop foot correction", *2013 IEEE/RSJ International Conference on Intelligent Robots and Systems*, 2013. Available: https://www.researchgate.net/profile/Mourad_Benoussaad/publication/259357581_Nonlinear_Model_Predictive_Control_of_Joint_Ankle_by_Electrical_Stimulation_For_Drop_Foot_Correction/links/02e7e52e615cf5fa12000000/Nonlinear-Model-Predictive-Control-of-Joint-Ankle-by-Electrical-Stimulation-For-Drop-Foot-Correction.pdf. [Accessed 20 March 2020].

[21] H. Lee, J. Lee and H. Kim, "Activities of ankle muscles during gait analyzed by simulation using the human musculoskeletal model", *Journal of Exercise Rehabilitation*, vol. 15, no. 2, pp. 229-234, 2019. Available:

https://www.e-jer.org/journal/view.php?number=2013600670&fbclid=IwAR2io5c_-DNg a8m2ViDcs0-sSvy1QFVXbNFf5f5GQGG6blyZHkSg7sRHeCU. [Accessed 20 March 2020].

[22] D. O'Keeffe, A. Donnelly and G. Lyons, "The development of a potential optimized stimulation intensity envelope for drop foot applications", *IEEE Transactions on Neural Systems and Rehabilitation Engineering*, vol. 11, no. 3, pp. 249-256, 2003. Available: https://www.ncbi.nlm.nih.gov/pubmed/14518788. [Accessed 20 March 2020].

[23] T. Kesar and S. Binder-Macleod, "Effect of frequency and pulse duration on human muscle fatigue during repetitive electrical stimulation", *Experimental Physiology*, vol. 91, no. 6, pp. 967-976, 2006. Available: https://physoc.onlinelibrary.wiley.com/doi/pdf/10.1113/expphysiol.2006.033886. [Accessed 30 March 2020].